AIAA JOURNAL
Vol. 48, No. 11, November 2010

Improved Algorithm for Nonlinear Sound Propagation with Aircraft and Helicopter Noise Applications

Seongkyu Lee,* Philip J. Morris,† and Kenneth S. Brentner‡
Pennsylvania State University, University Park, Pennsylvania 16802

DOI: 10.2514/1.J050396

An efficient numerical method to solve nonlinear sound propagation is presented. The frequency-domain Burgers equation, which includes nonlinear steepening and atmospheric absorption, is formulated in the form of the real and imaginary parts of the pressure. The new formulation effectively eliminates possible numerical issues associated with zero amplitude at higher frequencies occurring in a previous frequency-domain algorithm. In addition, to circumvent a high-frequency error that can occur in the truncated higher frequencies, a split algorithm is developed, in which the Burgers equation is solved below a cutoff frequency and a recursive analytic expression is used beyond the cutoff frequency. Finally, the Lanczos smoothing filter is incorporated to remove the Gibbs phenomenon. The new method is found to successfully eliminate high-frequency numerical oscillations and to provide excellent agreement with the exact solution for an initially sinusoidal signal with only a few harmonics. The new method is applied to a broad range of applications with a comparison to other methods to assess the robustness and numerical efficiency of the method. These include sonic boom, broadband supersonic jet engine noise, and helicopter high-speed impulsive noise. It is shown that the new method provides the fastest and most accurate predictions compared to the other methods for all the application problems.

Nomenclature

A	=	amplitude of the Fourier transform pressure, Pa s
B_n	=	nth harmonic amplitude
c	=	blade chord length, m
c_0	=	speed of sound, m s^{-1}
D_j	=	jet exit diameter, m
f	=	frequency of the acoustic signal, Hz
f_c	=	cutoff frequency, Hz
f_0	=	fundamental frequency of the sinusoidal signal, Hz
k	=	wave number, m^{-1}
M	=	Mach number
M_a	=	u_a/c_0, u_a is the peak particle velocity at the source, $M_a = p_a/\rho_0 c_0^2$
m	=	parameter for plane, cylindrical, and spherical waves
n	=	index of harmonic
p	=	acoustic pressure, Pa
$\tilde{p}$	=	Fourier transform of the pressure, Pa s
p_a	=	initial pressure amplitude of the sinusoidal wave, Pa
Q	=	amplitude of the Fourier transform of the pressure square, Pa^2 s
q	=	acoustic pressure squared, Pa^2
$\tilde{q}$	=	Fourier transform of the pressure square, Pa^2 s
R	=	rotor blade radius, m
r	=	propagation distance, m
r_f	=	final distance for the sound propagation, m
r_i	=	initial or starting distance for the sound propagation, m
U	=	real part of the Fourier transform of the pressure square, Pa^2 s
V	=	imaginary part of the Fourier transform of the pressure square, Pa^2 s
X	=	real part of the Fourier transform of the pressure, Pa s
$\bar{x}$	=	shock formation distance, m
Y	=	imaginary part of the Fourier transform of the pressure, Pa s
α	=	atmospheric absorption, neper m^{-1}
α'	=	atmospheric absorption and dispersion, $\alpha + i\beta_d$, m−1
β	=	coefficient of nonlinearity
β_d	=	atmospheric dispersion, m^{-1}
γ	=	ratio of the specific heats
δ	=	diffusivity of sound, m^2 s^{-1}
ε	=	nonlinear coefficients, $\beta/\rho_0 c_0^3$, kg^{-1} s
ρ_0	=	density, kg m^{-3}
σ	=	dimensionless propagation distance, $x/\bar{x}$
τ	=	retarded time, s
ϕ	=	phase of the Fourier transform of the pressure, rad
ψ	=	phase of the Fourier transform of the pressure square, rad
ω	=	angular velocity, rad/s

Presented as Paper 2010-1384 at the 48th AIAA Aerospace Sciences Meeting, Orlando, FL, 4–7 January 2010; received 20 December 2009; revision received 5 May 2010; accepted for publication 25 May 2010.

*Postdoctoral Research Associate, Department of Aerospace Engineering; currently Mechanical Engineer, General Electric Global Research Center, 1 Research Circle, Niskayuna, NY 12309; seongkyu.lee@ge.com. Member AIAA.

†Boeing/A. D. Welliver Professor, Department of Aerospace Engineering; pjm@psu.edu. Fellow AIAA.

‡Professor, Department of Aerospace Engineering; ksbrentner@psu.edu. Associate Fellow AIAA.

Introduction

ACOUSTIC waves can propagate nonlinearly for high-amplitude sound, causing a distortion of the waveform, eventually resulting in shocks, and then involving the dissipation of sound energy due to the shock wave. The waveform and amplitude of nonlinear sound are substantially different from those of linear sound. In addition, the nonlinear effect is cumulative and its importance increases for long distances.

One-dimensional nonlinear propagation can be described with the Burgers equation [1], which includes nonlinear steepening and atmospheric absorption. Previously, a mixed method [2,3] had been developed to calculate the propagation of a periodic wave and broadband jet engine noise. This method predicts the nonlinear steepening in the time domain from the Earnshaw solution and the atmospheric absorption effects in the frequency domain. The technique requires a resampling of the time history at every step, because the Earnshaw solution does not give the waveform at equal time spacings. The pressure resampling can modify some of the statistical properties of the waveform. Recently, a new nonlinear frequency-domain algorithm (NLFDA) for nonlinear propagation has been developed [4].

This method eliminates the need to resample the pressure signal. The method is also different from other frequency-domain methods in that the method does not construct a series representation of the nonlinear terms. The algorithm automatically constructs the ordinary differential equations for the amplitude and phase of the frequency components by finding the Fourier transform of the pressure and its square. The method has been used to predict the nonlinear propagation of broadband jet engine noise. However, it has been found that the numerical algorithm has numerical issues associated with the occurrence of zero amplitudes at higher frequencies. More important, the NLFDA has been found to exhibit numerical oscillations at high frequencies. This numerical error is more evident when a smaller number of harmonics are used. Because of the characteristics of nonlinear propagation, this numerical error occurring at high frequencies eventually contaminates solutions at all frequencies with increasing propagation distance when the nonlinear effect dominates the atmospheric absorption. In the present paper an improved algorithm to solve the nonlinear frequency-domain Burgers equation is introduced. It achieves robust and efficient predictions by eliminating the numerical issues associated with the previous algorithms. It is also shown to be more efficient.

Nonlinear acoustic theory has widespread practical applications in the areas of sonic boom and broadband engine noise. Little work, however, has been conducted on the nonlinear propagation of helicopter high-speed impulsive (HSI) noise. The nonlinear sound propagation of helicopter noise has been investigated mainly in the framework of computational fluid dynamics (CFD) and the acoustic analogy approach [5,6]. This approach is not appropriate to solve for the long-range propagation of HSI noise, since the approach cannot distinguish the nonlinear source and nonlinear propagation terms. Then all the nonlinearity is included in the source calculation, requiring a large extension of the CFD domain. It would be a better approach to separate the physical characteristics of HSI noise between nonlinear source and nonlinear propagation terms. The latter, in turn, is independently and efficiently solved by the Burgers equation model to large distances, while the former is accurately obtained by CFD in the near field. In the current paper, the new frequency-domain Burgers equation model is applied to a wide range of applications including sonic boom, broadband jet engine noise, and helicopter HSI noise to investigate the robustness and efficiency of the new algorithm compared to other numerical algorithms.

Generalized Burgers Equation and Numerical Method

New Nonlinear Frequency-Domain Algorithm

The generalized Burgers equation is written as [1]

$$\frac{\partial p}{\partial r}+\frac{m}{r}p-\frac{\delta}{2c_0^3}\frac{\partial^2 p}{\partial \tau^2}=\frac{\beta p}{\rho_0 c_0^3}\frac{\partial p}{\partial \tau} \tag{1}$$

where p is the acoustic pressure, β is the coefficient of nonlinearity, and δ is the diffusivity of sound:

$$\nu\left(\frac{4}{3}+\frac{\mu_B}{\mu}+\frac{\gamma-1}{Pr}\right)$$

The parameter m is equal to 0, 1/2, and 1 for plane, cylindrical, and spherical waves, respectively. For perfect gases, $\beta=(\gamma+1)/2$, and for diatomic gases such as air, $\gamma=1.4$ and therefore $\beta=1.2$. Note that τ in Eq. (1) is the retarded time, $\tau=t-r/c_0$. So the time history of the pressure at each range step is observed in a coordinate system moving with the speed of sound.

Equation (1) can be rewritten as

$$\frac{\partial p}{\partial r}+m\frac{p}{r}-\frac{\varepsilon}{2}\frac{\partial q}{\partial \tau}=\frac{\delta}{2c_0^3}\frac{\partial^2 p}{\partial \tau^2} \tag{2}$$

where $\varepsilon=\beta/\rho_0 c_0^3$, and the square of the pressure is represented by $q(r,\tau)$. The Fourier transform of Eq. (2) yields

$$\frac{\mathrm{d}\tilde{p}}{\mathrm{d}r}+m\frac{\tilde{p}}{r}+\alpha'\tilde{p}=\frac{i\omega\varepsilon}{2}\tilde{q} \tag{3}$$

where $\tilde{p}$ and $\tilde{q}$ are the Fourier transform of the pressure and pressure square, respectively. $\omega^2\delta/2c_o^3$ has been replaced with α', the atmospheric absorption. When dispersion effects are important, they are included in α' such that the absorption becomes a complex variable, $\alpha'=\alpha+i\beta_d$. The real part of the complex coefficient α' is associated with attenuation and can be obtained by the method presented by Bass et al. [7,8]. A formula for the imaginary part describing the dispersion effects and their variation with frequency is given in [3,4]. Finally, Eq. (3) can be expressed as two ordinary differential equations for the amplitude and phase [4], respectively:

$$\frac{\mathrm{d}A}{\mathrm{d}r}=-\frac{A}{r}-\frac{\omega\varepsilon Q}{2}\sin(\psi-\phi)-\alpha A \tag{4a}$$

and

$$\frac{\mathrm{d}\phi}{\mathrm{d}r}=\frac{\omega\varepsilon Q}{2A}\cos(\psi-\phi)-\beta_d \tag{4b}$$

where A and Q represent the amplitude of the pressure and pressure square, respectively, and ϕ and ψ represent the phase of the pressure and pressure square, respectively.

These ordinary differential equations can be solved by any marching scheme. Here, a second-order Runge–Kutta scheme has been used to find the amplitude $A(r+\delta r,\omega)$ and phase $\phi(r+\delta r,\omega)$ of the pressure at the next range step at each frequency. The inverse Fourier transform is used to find the pressure in the time domain and then the square of the pressure is calculated. The amplitude and phase of the Fourier transform of the pressure and the pressure square are then used to find the amplitude and phase of the pressure at the next range step. The whole process is then repeated until the required distance is reached. This numerical algorithm with Eq. (4) was designated as the NLFDA method [4].

However, Eq. (4) has some numerical issues. First, Eq. (4a) has a possibility of a negative magnitude if the previous magnitude at a specific frequency is zero and the sine function is positive. In addition, Eq. (4b) implies the possibility of a singularity when the amplitude at certain frequencies is zero. A very large numerical error associated with the phase singularity affects the integration of the magnitude Eq. (4a) in the next step so that the error accumulates as the integration continues. These problems are found to occur when the starting point is situated close to the source and higher frequencies due to nonlinear effects are not sufficiently populated. To circumvent these numerical problems, the NLFDA method uses an ad hoc correction in which the inverse Fourier transform of the magnitude and phase obtained by Eq. (4) yields the pressure–time history and then the Fourier transform of the pressure offers a new magnitude and phase that have reasonable, though not necessarily correct, values. This process is found to regularize the values of the magnitude and phase. The corrected magnitude and phase are used to find the magnitude and phase at the next range step. Even though this magnitude and phase correction has been found to provide accurate results, it increases computation time due to additional calculations of the inverse and direct Fourier transforms at each range step and, as shown next, it is unnecessary.

A new numerical algorithm to solve the frequency-domain Burgers equation is proposed in the present paper. The pressure and pressure square are expressed in the form of complex variables:

$$\tilde{p}(r,\omega)=X+iY \tag{5}$$

and

$$\tilde{q}(r,\omega)=U+iV \tag{6}$$

Then Eq. (3) can be expressed as

$$\frac{\mathrm{d}(X+iY)}{\mathrm{d}r}+m\frac{(X+iY)}{r}+(\alpha+i\beta_d)(X+iY)=\frac{i\omega\varepsilon}{2}(U+iV) \tag{7}$$

The separation of Eq. (7) into its real and imaginary parts gives

$$\frac{dX}{dr} = -m\frac{X}{r} - (\alpha X - \beta_d Y) - \frac{\omega\varepsilon}{2}V \tag{8a}$$

$$\frac{dY}{dr} = -m\frac{Y}{r} - (\beta_d X + \alpha Y) + \frac{\omega\varepsilon}{2}U \tag{8b}$$

At every range step, U and V are computed from the pressure square. Note that Eq. (8) has neither the negative amplitude nor the phase singularity issues, which were present in the original NLFDA Eq. (4). Therefore, this algorithm works for a signal that has initially zero amplitudes at the higher frequencies without causing an error. Since the ad hoc correction is no longer needed, this new algorithm also avoids the associated increase in computation time.

It is worthwhile to note that the ordinary differential equations with respect to the real and imaginary parts of the pressure in the frequency domain have been presented in previous work [9]. However, Eq. (8) is different from the previous work in that it does not involve series representation for the pressure squared. Instead, the pressure squared in the frequency domain is also expressed in terms of its real and imaginary parts. Therefore, the expression used in the new algorithm is simpler and the computation is more efficient than for other frequency-domain algorithms.

Elimination of High-Frequency Errors

The frequency-domain nonlinear propagation method described in Eq. (4) or Eq. (8) has been found to experience numerical oscillations at high frequencies. The energy flow from the lower to higher frequencies is limited by the highest resolved frequency. In reality, all the frequencies beyond the highest resolved frequency should have some amplitude. Since the frequency resolution is limited, an error occurs at the highest frequency and this gradually contaminates the lower frequency range as the sound propagates. To minimize the effect of this numerical error on the time signal, a very large number of harmonics would be needed, which increases the computational cost.

Pishchal'nikov et al. [10] proposed a new method to avoid a large number of harmonics to represent shock wave. They solved the low-frequency components by using the Burgers equation and determined the high-frequency components analytically subject to an appropriate matching condition. The amplitude and phase of the high-frequency components are calculated with a matching condition that is a function of the highest two frequency components determined numerically by the Burgers equation. An asymptotic solution for the high-frequency components is used to determine the pressure at the lower frequency components through the series summation. In the current paper, the same idea of using a high-frequency asymptotic solution is used. The low-frequency components are solved by the Burgers equation and the high-frequency components are obtained by an analytic solution describing a discontinuity, such as an N-wave. However, the current paper does not use a series summation, as discussed earlier, and the numerical implementation is much simpler. The asymptotic solutions are found for the high-frequency components and these high-frequency solutions are used, along with low-frequency solutions obtained by the Burgers equation, to construct the pressure–time history through the inverse Fourier transform.

In the sawtooth region of a periodic signal, the waveform can be represented by the following Fourier series:

$$p = \frac{2p_0}{1+\sigma}\sum_{n=1}^{\infty}\frac{1}{n}\sin n\omega\tau \tag{9}$$

That is, the harmonic amplitudes are $B_n = 2/n(1+\sigma)$, where σ represents a dimensionless propagation distance whose definition will be given later. Clearly, the ratio of the amplitudes of adjacent frequency components is given by

$$B_n = B_{n-1} \times \frac{n-1}{n} \tag{10}$$

or

$$\left|\frac{\tilde{p}((n-1)\omega_0)}{\tilde{p}(n\omega_0)}\right| = \frac{n-1}{n} \tag{11}$$

where $|\tilde{p}(\omega)|$ is the amplitude of the pressure at frequency of ω. In the present implementation a cutoff frequency f_c is chosen. Typically, this is at a very high frequency or harmonic. If the pressure amplitude at the frequency above f_c is greater than the value at the adjacent lower frequency or harmonic, its amplitude is determined from a recurrence relation given by Eq. (11).

Instead of solving for the amplitude at all frequencies using the frequency-domain Burgers equation, Eq. (11) is used to find the amplitude of the frequencies beyond the cutoff frequency recursively when the amplitude does not decrease with frequency. This split frequency-domain method is based on the assumption that energy should decrease as the frequency increases beyond a given cutoff frequency. By doing this, nonphysical growth at high frequencies can be successfully eliminated. It has been found that the method is not sensitive to the value of the cutoff frequency f_c, as long as a suitably large value of f_c is selected. Although this technique has been formulated for a periodic wave, its validity for real applications such as broadband jet noise, sonic boom, and helicopter noise will be demonstrated later.

Since a shock wave consists of many harmonics of nonzero values, the truncation of harmonics causes the Gibbs phenomenon, or oscillations at the peaks. Computation far beyond the audible frequency range causes excessive computational cost. As a second process to cure high-frequency errors associated with this Gibbs phenomenon, the Lanczos smoothing filter [11] is employed at the last range step. This process effectively eliminates the Gibbs phenomenon and achieves an accurate prediction using fewer harmonics.

A frequency-domain Burgers equation given in the form of the real and imaginary parts of the pressure, as shown in Eq. (8), with a mix of frequency-domain marching with analytical extensions for the highest unresolved frequencies and with the Lanczos smoothing filter is referred to as the *split method* in the present paper.

Validation Problem

In this section, an initially sinusoidal wave is used to validate the numerical method against an exact solution. The initial sine wave is given by

$$p(r,\tau) = p_a \sin(2\pi f_0 \tau) \tag{12}$$

The parameters p_a and f_0 are chosen to be 140 dB re 20 μPa (or 282.84 Pa) and 1000 Hz, respectively.

The shock formation distance for a plane sinusoidal wave is given by

$$\bar{x} = \frac{1}{\beta M_a k} \tag{13}$$

where β is the coefficient of nonlinearity, M_a is u_a/c_0, u_a is the peak particle velocity at the source, and k is the wave number. M_a is given by $p_a/\rho_0 c_0^2$ [1]. The speed of sound and density are chosen to be 343 m/s and 1.213 kg/m^3, respectively. A dimensionless parameter $\sigma = x/\bar{x}$ is used to define the propagation distance. The shock formation distance for the sine wave corresponds to $\sigma = 1$ (22.90 m for the current simulation). $\sigma = 3$ is chosen for a benchmark problem in this paper. (Although not shown, both the NLFDA and split methods have been found to provide excellent agreement with the exact solution in the preshock region.) An analytic solution for the transition region between the preshock and sawtooth regions, i.e., $1 < \sigma < 3$, can be obtained from the Blackstock bridging function (BBF) solution [1].

Figure 1 shows comparisons of the normalized pressure–time history and the sound pressure level (SPL) for the BBF solution with 256 harmonics and predictions obtained by the NLFDA method at $\sigma = 3$. The exact solution uses the Lanczos filter to eliminate the Gibbs phenomena. The prediction uses three different numbers of harmonics (NH = 32, 64, 256). To match zero crossing points with the BBF solution, the dispersion coefficient is set to be zero in the

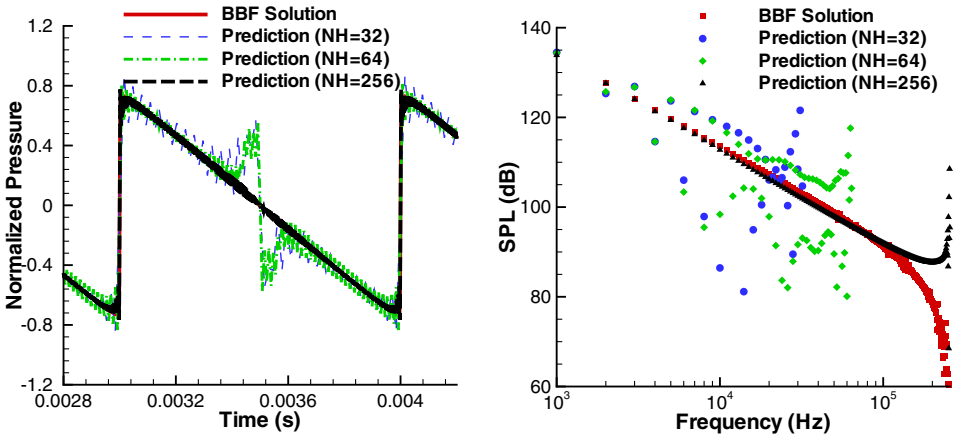

Fig. 1 Comparison between the BBF solution and predictions obtained by the NLFDA method for various numbers of harmonics: a) the normalized pressure–time history and b) sound pressure level. For the exact solution, only the 256-harmonic result is shown.

prediction, but a nonzero absorption coefficient is used. It can be seen that large numerical oscillations occur in the pressure–time history. These are associated with high-frequency errors as described earlier. These high-frequency errors move to lower frequencies as the sound propagates, resulting in significant errors in the lower harmonics. This gives the extra oscillations seen in Fig. 1 for the 32- and 64-harmonic cases. As the number of harmonics increases, the numerical oscillations are reduced and the predicted waveform approaches the exact solution. But the numerical oscillations still exist and this numerical error would gradually grow with increasing propagation distance. In addition, the use of a large number of harmonics, which may be far beyond the audible frequency range, is not desirable in terms of computational efficiency. The result presented in [4] does not show this abnormal behavior, as the last few high harmonics were simply removed when the pressure–time history was recovered. However, it results in a discrepancy of the slope between the analytic solution and the prediction.

Figure 2 shows the predictions obtained by the new split method. The cutoff frequency is selected as 90% of the Nyquist frequency for each harmonic case. It can be seen that predictions with NH = 32 and 64 provide very good agreement with the BBF solution for the pressure waveform without introducing the numerical oscillations. It appears that 30 to 50 harmonics are sufficient to describe the shock waveform accurately for this waveform, so calculations beyond these harmonics are simply additional computational cost. It should be noted that only the 256-harmonic result is shown for the exact solution. The Lanczos filter was used for both the exact solution and predictions. This result illustrates that the proposed method improves the nonlinear propagation frequency-domain algorithm significantly and enables an efficient and accurate numerical prediction.

Figure 3 shows the effect of the Lanczos filter for the 64-harmonic case in the prediction with the new split method. It can be seen that the highest resolved frequency has a large amplitude when the filter is not used. This can be described as the Gibbs phenomena, oscillations in the shock corners, in the time domain. However, the Lanczos filter dramatically reduces the high-frequency amplitudes so that the Gibbs phenomena is completely removed, providing smooth corners of the shock.

Nonlinear Propagation of Sonic Boom

In this section, predictions of the nonlinear propagation of a sonic boom are compared. These cases are chosen to illustrate the improved accuracy and efficiency of the new split method. Cleveland et al. [12] compared computer codes for the propagation of sonic boom waveforms through isothermal atmospheres. The same benchmark problem is used to validate the present method for sonic boom. Two test waveforms, referred to here by the names flattop and ramp, were generated by the NASA Langley Research Center for sonic boom studies. They are representative of a class of low boom waveforms with additional features to challenge the codes. The flight altitude is specified to be 14,630 m (48,000 ft) and the Mach number is 1.8. The test waveforms are given at a distance of 183 m (600 ft) below the aircraft. In the test case, the sound speed is not a function of altitude. Acoustic rays therefore travel in straight lines, and the geometrical spreading is simply cylindrical. The waveforms have

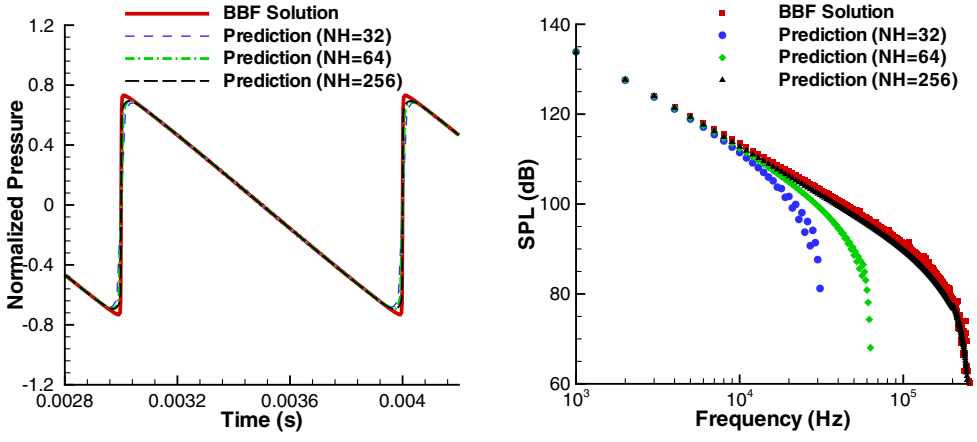

Fig. 2 Comparison between the BBF solution and predictions obtained by the split method for various numbers of harmonics: a) the normalized pressure–time history and b) sound pressure level. For the exact solution, only the 256-harmonic result is shown.

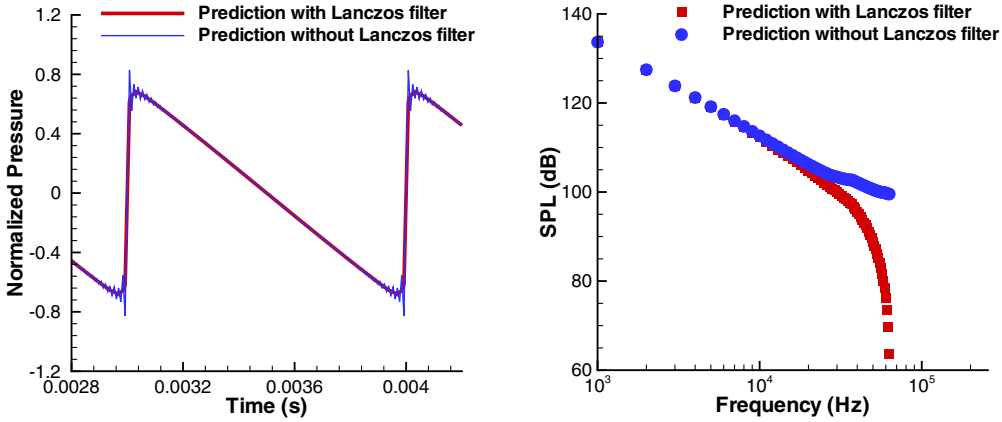

Fig. 3 Effect of the Lanczos filter: a) the normalized pressure–time history and b) sound pressure level. 64 harmonics are used.

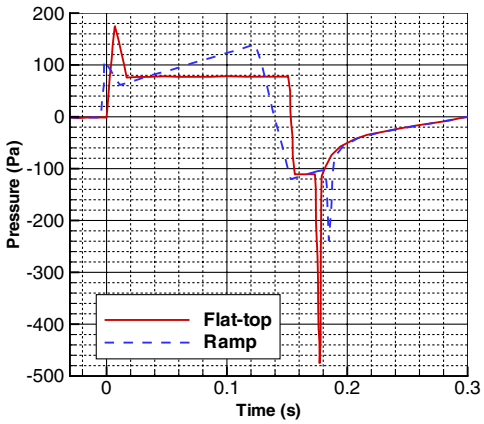

Fig. 4 The two initial source waveforms, the flattop and ramp, used for sonic boom.

been digitized from the figure of the original reference [12] and then interpolated with a uniform time step. Figure 4 shows the flattop and ramp test waveforms. The atmospheric conditions are ambient temperature $T = 273.15$ K, ambient pressure $P = 1$ atm. A relative humidity of 20% was specified.

Figure 5 shows a comparison of predicted ground waveforms of the flattop waveform for nonlinear propagation predictions and linear propagation in the uniform atmosphere. Three different numerical algorithms are used for the nonlinear predictions: 1) the NLFDA method, 2) the split method, and 3) the mixed frequency- and time-domain method. The mixed method is the algorithm that calculates the nonlinear steepening in the time domain and determines the atmospheric absorption and dispersion in the frequency domain [2,3]. In the split method, the cutoff frequency is set to be 20 kHz. The number of sampling time steps (NT), which is the number of data points in the pressure–time signal, used to characterize the waveform in the predictions, is 2048. The shock waves of the bow and trailing waves are apparent in the figure. Three nonlinear propagation predictions provide similar results, but the mixed method gives a slightly different amplitude and phase for the tail boom. This discrepancy is found to be due to the mixed method requiring a large number of time steps to obtain the fully converged result. This will be discussed in the next paragraph. The results for the ramp signal are shown in Fig. 6. The NLFDA and split methods provide almost the same prediction, while the mixed method results in slightly reduced amplitude at the tail boom.

Table 1 shows the parameters and computation time to obtain the converged results for both flattop and ramp booms for the three numerical algorithms. For the given number of time sampling steps (NT), the number of range steps from the starting position to the final distance (NR) is increased until a converged solution is obtained for all methods. This process is repeated when NT is increased. Therefore, NT and NR are determined to obtain the converged solution in terms of both time sampling steps and range steps. It is found that the NLFDA method and the split method provide a converged result with NT = 2048, while the mixed method requires a much larger number of sampling time steps, NT = 65536, to obtain the converged result for both the flattop and ramp booms. As a result, the split method achieves a reduction in computation time by a factor of 100 compared to the mixed method for the flattop case. When the

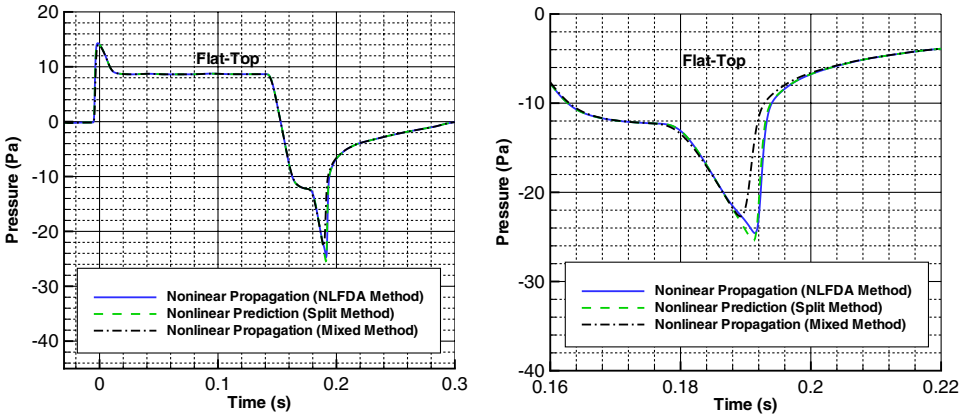

Fig. 5 Predicted ground waveforms of the flattop boom in the uniform atmosphere with full atmospheric absorption and dispersion (relative humidity 20%): a) the entire boom shape and b) an enlarged figure around the tail boom.

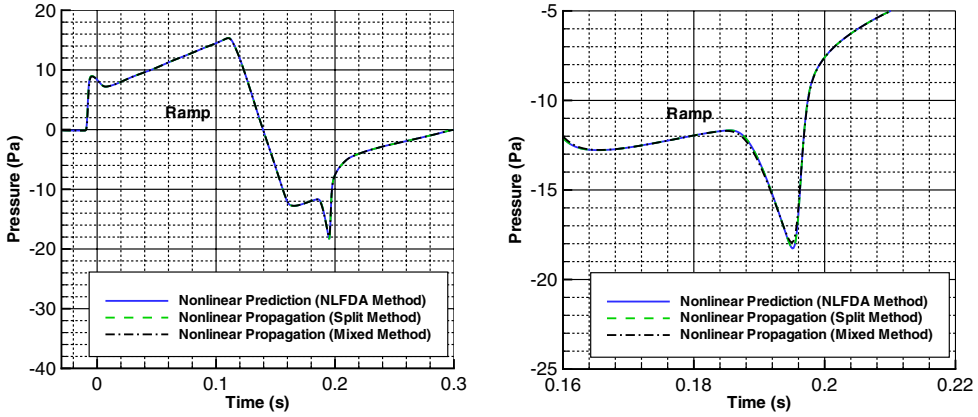

Fig. 6 Predicted ground waveforms of the ramp boom in the uniform atmosphere with full atmospheric absorption and dispersion (relative humidity 20%): a) the entire boom shape and b) an enlarged figure around the tail boom.

Table 1 Convergence test of nonlinear propagation predictions for flattop and ramp booms[a]

	NT	NR	Time
Flat top			
NLFDA method	2,048	20,000	19.6 s
Split method	2,048	7,000	3.8 s
Mixed method	65,536	27,991 ($\eta = 0.005$)[a]	398 s
Ramp			
NLFDA method	2,048	2,000	2.1 s
Split method	2,048	2,000	1.2 s
Mixed method	65,536	2,749 ($\eta = 0.005$)[a]	39.7 s

[a]η is a parameter for determining an adaptive range step employed in the mixed method such that $\mathrm{d}r = \eta\rho_0 c_0^3/\beta(\mathrm{d}p/\mathrm{d}t)_{\max}$.

split method is compared with the NLFDA method, it can be seen that the NLFDA method requires a larger number of the range steps NR than the split method for the flattop case. The gain of computational savings with the split method compared to the NLFDA method is a factor of 5 for the flattop case. It is worth noting that both the NLFDA method and split method require the same NT and NR for the ramp case, but the split method reduces computation time by one-half. This is because the split method does not involve the ad hoc magnitude and phase correction as described earlier. All in all, the benefit of the split method in terms of computation time is evident. In addition, it can be seen that computation times for the flattop case are much longer than for the ramp case. This is because the flattop contains stronger shock waves for both the front and tail booms than for the ramp. This required a larger number of range steps to obtain the converged solutions for the flattop case compared to the ramp case. Figure 7 shows the tail boom with increasing NT for the split method and mixed method for the flattop and ramp booms. It can be seen that the results obtained by the split method do not vary with the sampling time steps, while the results obtained by the mixed method approach that of the split method with increasing NT. The converged results are also indistinguishable for the split method.

Broadband Supersonic Jet Noise

Broadband jet-noise data obtained from the Boeing Low Speed Aeroacoustic Facility (LSAF) for a supersonic heated jet with $M = 1.9$ are used to assess the nonlinear sound propagation of broadband aircraft engine jet noise [13]. The atmospheric conditions for the experiment are shown in Table 2.

The data were originally sampled at 192 kHz with 79,801 points and have been truncated to 2^{16} or 65,536 points. The pressure signal is propagated from the initial measurement location of 100 D_j from the jet exit, where D_j is the jet exit diameter of 3.23 cm. Ensemble averaging with 1024 segment points, 50% overlap, and a Hanning Window are used to generate broadband SPL.

Figure 8 shows the SPL and the difference between measurement and predictions at the 289D_j location. In the split method, the cutoff frequency is set to be 90 kHz. Linear propagation is also shown in the figure. The NLFDA method results in a slightly higher SPL at high frequencies. It can be seen that the mixed method does not capture the high-frequency rise and it gives almost the same result as for linear propagation. The discrepancy between the mixed method and the measurement at high frequencies for the Boeing LSAF subsonic case

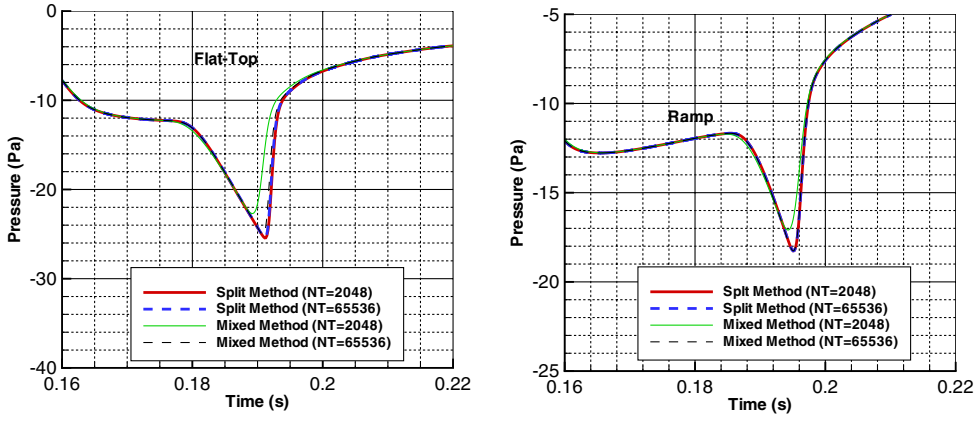

Fig. 7 Comparison of the split method and mixed method for two numbers of time step: NT = 2048 and 65,536.

Table 2 Atmospheric conditions for Boeing LSAF supersonic measurement

Conditions	Values
Temperature, K	282.87
T_j/T_a	2.84
Atmospheric pressure, atm	0.99483
Relative humidity, %	68.6

is also discussed by Gee [3]. Although he attributed the discrepancy to measurement error, it is thought that it is the mixed method that fails to capture the high-frequency rise for the current case, since the other methods capture the high-frequency rise well. The discrepancy in the mixed method may also be due to the fact that the method is not fully converged in terms of the sampling frequency as indicated by the sonic boom problem. It can been seen that the split method provides the best agreement with the measured data. It should be noted that the nonlinear result is 5 dB higher than the linear result at high frequencies. The discrepancy at relatively low frequencies, around 1 kHz, is thought to be due to the distributed sources at the rear of the jet exit. In the Burgers equation, all noise sources are assumed to be concentrated as a single point is the jet exit. This can be acceptable for high-frequency noise sources, but low-frequency sources are much more distributed along the jet axis.

A final distance of 2000 D_j is considered to investigate the cumulative effect of nonlinear propagation for large distances. However, there is no measurement data available at this distance, so the results are used to assess the robustness of the methods. Figure 9 shows a comparison of the nonlinear propagation predictions and a linear propagation prediction. It can be seen that the SPL of the mixed method prediction lies between the linear propagation and the split method, which is consistent with the near-field prediction. The NLFDA method clearly overpredicts the nonlinear effects at high frequencies beyond 30 kHz. This might be due to the accumulation of the high-frequency error with increasing distance and the error becomes more pronounced for long distances. Again, the split method appears to provide a reasonable prediction based on the convergence test performed in the previous section.

Helicopter High-Speed Impulsive Noise

In this section, nonlinear propagation of helicopter high-speed impulsive noise is addressed. High-speed impulsive (HSI) noise is a particularly intense and annoying noise generated by helicopter rotors in high-speed forward flight [14]. HSI noise is closely associated with the appearance of shocks and transonic flow around the advancing rotor blades. This HSI noise generally occurs with advancing tip Mach number above $M_{\mathrm{AT}} = 0.85$. HSI waveforms experience significant nonlinear steepening as the propagation distance increases.

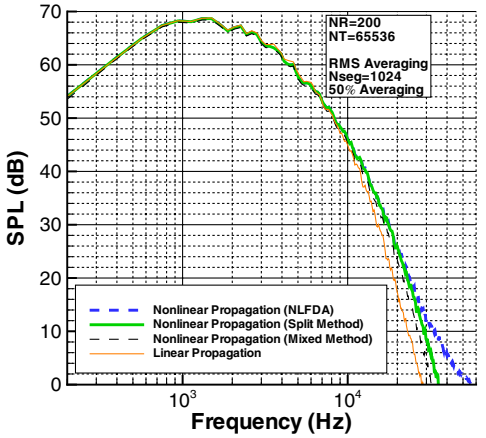

Fig. 9 Predictions for Boeing LSAF supersonic heated jet at 2000 D_j.

A model scale rotor test, conducted by Boxwell et al. [15] in 1978 and later repeated by Purcell [16] in 1988, has been selected for the validation of the present analysis and code. The rotor was a one-seventh-scale model of a UH-1H main rotor with straight, untwisted, blades. The model rotor had an NACA 0012 airfoil section. The rotor radius R was 1.045 m with a chord of 7.62 cm. The model was run at several high-speed hover conditions with low thrust. An Euler solution reported by Baeder et al. [17] was used to extract the starting signal. The Euler calculation was performed on a C-H grid in the blade-fixed frame, where the blade is fixed and the flow is rotating; the only used grid was the lower half of the flow volume in the CFD calculations by taking advantage of the symmetry of the problem. Details of the Euler calculations can be found in [17,18]. In this paper, only the hovering case with a tip Mach number of 0.95 is considered.

The numerical solution of the Burgers equation requires the starting and the final distances, r_i and r_f, respectively. Menounou and Vitsas [19] used the Burgers equation model to predict nonlinear propagation of helicopter blade–vortex-interaction noise. They assumed that the noise is emitted from the rotor hub center so that r_i and r_f are measured from the hub center to the starting point and the observer, respectively. This simple assumption would lead to a false directivity pattern, since the propagation path is not correct. In the present paper, HSI noise is considered and parameters for the propagation are found by a geometrical consideration of the propagation path. Figure 10 shows a density contour normalized by the ambient density obtained by the CFD around a rotor blade for a hovering tip Mach number of 0.95. It is shown that the disturbance follows the characteristic curve in the blade-fixed frame. The characteristic curve is considered as a wave front moving outward in the inertial frame. In the figure, sound is assumed to be generated at the blade tip $A(x/c, y/c) = (14.14, 0.11)$ and propagates toward

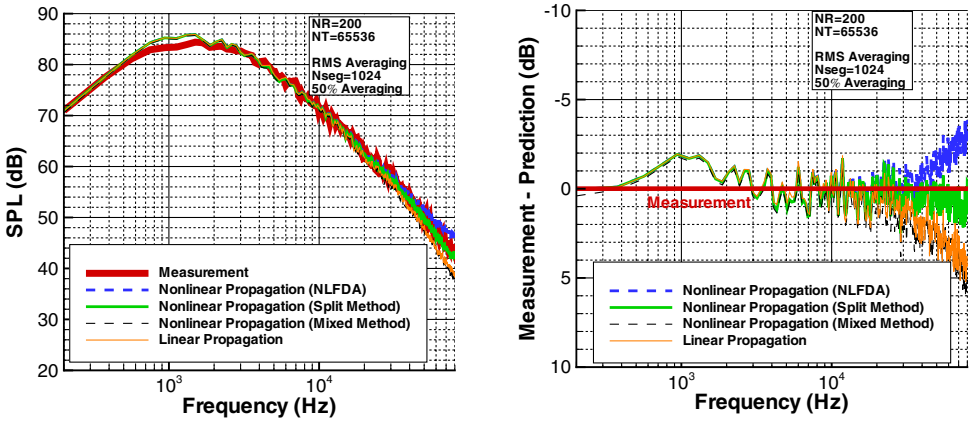

a) b)

Fig. 8 Sound pressure level for experimental data and predictions for Boeing LSAF supersonic heated jet at 289 D_j.

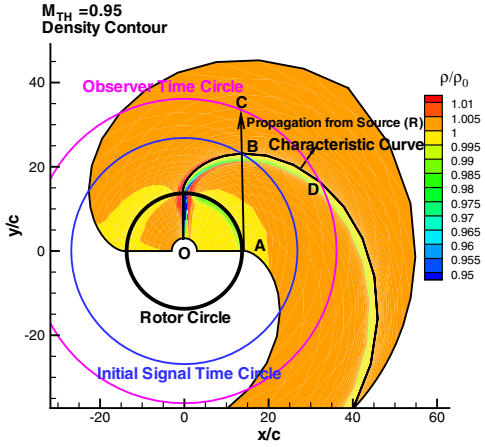

Fig. 10 Schematic of nonlinear propagation of rotor noise using the CFD data for the starting signal for a UH-1H model rotor with a hovering tip Mach number of 0.95.

points $B(x/c, y/c) = (13.62, 23.14)$ and $C(x/c, y/c) = (13.30, 33.51)$ (where c is the chord length), resulting in $r_i = 1.76$ m and $r_f = 2.55$ m or $r/R = 2.63$ (where r is the distance from the origin and R is the blade radius). The initial data is extracted at B and then the signal is propagated to C using the Burgers equation model. This propagation path is described in the inertial frame. Note that the propagation line $\overline{ABC}$ is perpendicular to the tangential line of the characteristic curve at B. The pressure–time history obtained by the Burgers equation at C in the inertial frame should be equal to the pressure–time history obtained by the CFD at $D(x/c, y/c) = (32.25, 16.23)$ in the blade-fixed frame. The position D can be found by the intersection of the characteristic curve and a circle with the radius of $\overline{OC}$, where O is the rotor center. Then the pressure–time history at D is extracted from the CFD along the observer time circle. Note that the source position is assumed to be fixed. Normally, the variation of the source position is small so that the approximation is thought to be reasonable.

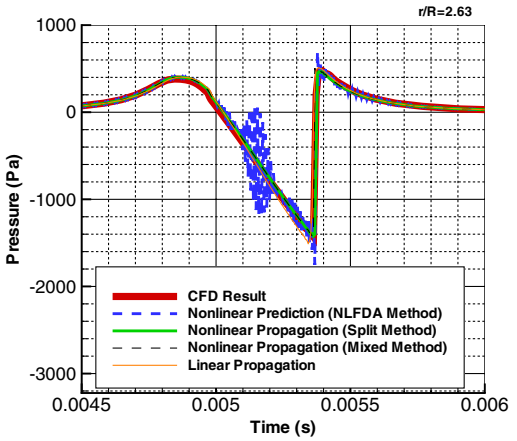

Fig. 11 Comparison of UH-1H model rotor noise at $r/R = 2.63$ with a hovering tip Mach number of 0.95.

Figure 11 shows a comparison of the predictions with the CFD result at $r_f = 2.55$ m. While the CFD is lossless, the temperature and relative humidity used for the atmospheric absorption and dispersion in the nonlinear prediction are chosen to be 293.15 K and 20%, respectively, and 2048 time steps in the pressure–time history are used in the prediction. It can be seen that the NLFDA method results in numerical oscillations due to the high-frequency error, even though these oscillations can be removed by increasing NT and dropping high frequencies, while the split method and mixed method provide fairly good agreement with the CFD result. The width of the wave, the negative peak, and the shock rise time are well predicted. A possible discrepancy between the nonlinear propagation result and the CFD result might be due to the assumption of the fixed source position, atmospheric absorption, and dispersion effect (which are not considered in the CFD); inaccuracies in the CFD; or the localized nonlinear effect, which is neglected in the Burgers equation. Collectively, those differences are very small and negligible. Linear propagation does not completely capture the part of the expansion wave between 0.005 and 0.0054 s and slightly overpredicts the negative peak.

Figure 12a shows a comparison of the predictions for long distance propagation ($r/R = 1000$). Linear propagation shows a discrepancy from the nonlinear propagation in the region of the main pulse between 0.004 and 0.006 s. It is interesting to note that the width of the main pulse (0.002 s) is much broader than that obtained in the near field (0.0004 s) of $r_f = 2.55$ m or $r/R = 2.63$. It is thought to be due to the nonlinear effect being superseded by atmospheric absorption so that the high-frequency energy is greatly dissipated. For the same reason, the high-frequency error occurring in the NLFDA method in the near field is no longer evident in the waveform at this large distance. As a result, the NLFDA method and the split method provide very similar results for nonlinear propagation. The mixed method, however, shows a large discrepancy of the waveform between the negative peak and the second positive peak. This error is found to be due to the fact that the mixed method does not provide a converged result with NT = 2048 as shown in Fig. 12b. As NT increases, the result obtained by the mixed method approaches that obtained by the split method. It should be noted, however, that NT does not change the split method result.

Table 3 shows the parameters and computation time needed to obtain the converged result for the three numerical algorithms. The

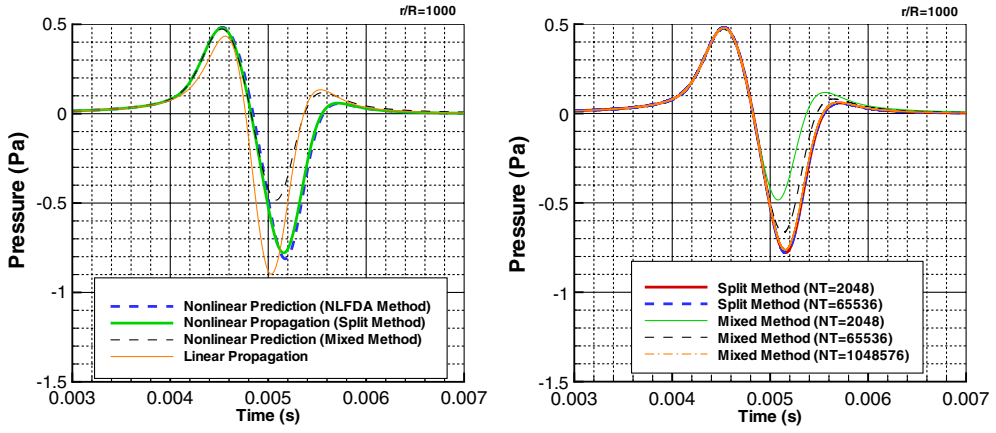

a) b)

Fig. 12 Comparison of UH-1H model rotor noise at $r/R = 1000$ m with a hovering tip Mach number of 0.95: a) comparison of predictions with 2048 time steps and b) the effect of the number of sampling time steps on the predictions.

Table 3 Convergence test of nonlinear propagation predictions for UH-1H model rotor noise at $r/R = 1000$ m with a hovering tip Mach number of 0.95

	NT	NR	Time
NLFDA method	2,048	150,000	155.83 s
Split method	2,048	30,000	17.46 s
Mixed method	1,048,576	$\eta = 0.005$[a]	81 h

[a]η is a parameter for determining an adaptive range step employed in the mixed method such that $dr = \eta\rho_0 c_0^3/\beta(dp/dt)_{\max}$.

mixed method requires a very large number of time samples and the computation time takes about 81 h, which is not practical for routine calculations. The NLFDA method and split method requires only 2048 time samples to obtain the converged result. Note that even though the NLFDA and split method provide almost the same waveform for NT = 2048, the convergence test demonstrates that the split method saves the computation time by a factor of 8 compared to the NLFDA method, since a smaller number of range steps are required to obtain the converged solution for the split method. The elimination of the ad-hoc process associated with numerical issues appeared in the NLFDA method also contributes to the reduction in time.

Conclusions

A new algorithm for nonlinear noise propagation has been developed for solving the generalized Burgers equation in the frequency domain. The new algorithm is formulated in the form of the real and imaginary parts of the pressure so that it ensures a more robust and efficient algorithm by eliminating some numerical issues associated with zero amplitude at higher frequencies occurring in the previous NLFDA algorithm. In addition, the new method effectively splits the numerical algorithm into two solution procedures to eliminate nonphysical high-frequency growth: 1) to solve the Burgers equation below a cutoff frequency, 2) to use the recursive analytic expression for the amplitude beyond the cutoff frequency. Finally, the Lanczos filter is implemented to the method to overcome the Gibbs phenomenon.

The new method, referred to as the split method, demonstrates excellent agreement with an analytic solution for an initially sinusoidal signal with only a relatively few harmonics without causing high-frequency oscillations. The method is then applied to sonic boom, broadband supersonic jet engine noise, and helicopter high-speed impulsive noise to assess the robustness and numerical efficiency. The split method is compared with two different numerical algorithms: the NLFDA method (the frequency-domain method that is formulated in terms of the amplitude and phase of the pressure and solves the Burgers equation at all frequencies) and the mixed method (the method that solves nonlinear distortion in the time domain and accounts for atmospheric absorption and dispersion in the frequency domain).

For sonic boom, it has been shown that the split method provides good converged results with a relatively small number of time samples, while the mixed method requires a large number of data points to obtain the same converged results. Even though the split method and the NLFDA method result in almost the same waveform, the split method achieves a large computational saving because it does not use an ad hoc process to eliminate the numerical issues associated with zero amplitude at high frequencies and it requires the smallest number of range steps. For broadband jet engine noise, nonlinear propagation gives a rise of high-frequency energy. The split method provided the best agreement with measured data, while the NLFDA method overpredicted and the mixed method underpredicted the high-frequency rise. In addition, the NLFDA method showed numerical errors in the high-frequency range for a distance of 2000 Dj. For helicopter HSI noise, the CFD data of the model helicopter rotor have been used for extracting the starting signal and for the validation of the nonlinear propagation predictions. A propagation path was found by using the characteristic curve in the CFD grid and geometrical consideration of the path. It has been found that the split method successfully eliminates high-frequency numerical oscillations that appear in the NLFDA prediction in the near field so that the prediction obtained by the split method agrees very well with the CFD data. For a large distance, the mixed method required a very large number of time samples to obtain the converged result, while the split method provides good convergence with a small number of time samples. A noticeable change in the waveform was seen between the nonlinear and linear propagations for a large distance. The present method is better suited to analyze the long-range propagation of helicopter HSI noise than the acoustic analogy approach, since the nonlinear propagation term is accurately and effectively calculated.

Overall, the present algorithm to solve the frequency-domain Burgers equation has been shown to be robust, accurate, and efficient for a broad range of applications.

Acknowledgments

This research is funded by the Government under agreement no. W911W6-06-2-0008 under the task of Vertical Lift Research Center of Excellence (VLRCOE) at Pennsylvania State University. The authors would like to thank K. Viswanathan for providing Low Speed Aeroacoustic Facility data.

References

[1] Hamilton, M. F., and Blackstock, D. T., *Nonlinear Acoustics*, Academic Press, New York, 1997.

[2] Anderson, M. O., "Propagation of a Spherical *N* Wave in an Absorbing Medium and Its Diffraction by a Circular Aperture," Applied Research Labs., Univ. of Texas at Austin, TR ARL-TR-74-25, Austin, TX, 1974.

[3] Gee, K. L., "Prediction of Nonlinear Jet Noise Propagation," Ph.D. Thesis, Graduate Program in Acoustics, Pennsylvania State Univ., University Park, PA, 2005.

[4] Saxena, S., Morris, P. J., and Viswanathan, K., "Algorithm for the Nonlinear Propagation of Broadband Jet Noise," *AIAA Journal*, Vol. 47, No. 1, 2009, pp. 186–194. doi:10.2514/1.38122

[5] Farassat, F., and Brentner, K. S., "Supersonic Quadrupole Noise Theory for High-Speed Helicopter Rotors," *Journal of Sound and Vibration*, Vol. 218, No. 3, 1998, pp. 481–500. doi:10.1006/jsvi.1998.1836

[6] Lee, S., Brentner, K. S., Hennes, C. C., Flynt, B. T., Theron, J. N., and Duque, E. P. N., "Investigation of the Accuracy Requirement for Permeable Surfaces Used in Rotor Noise Prediction," *62nd AHS Forum of the American Helicopter Society*, AHS International, Alexandria, VA, May 2006.

[7] Bass, H., Sutherland, L., Zuckerwar, A., and Blackstock, D., "Atmospheric Absorption of Sound: Further Developments," *Journal of the Acoustical Society of America*, Vol. 97, No. 1, 1995, pp. 680–683. doi:10.1121/1.412989

[8] Bass, H., Sutherland, L., Zuckerwar, A., and Blackstock, D., "Erratum: Atmospheric Absorption of Sound: Further Developments," *Journal of the Acoustical Society of America*, Vol. 99, No. 2, 1996, p. 1259. doi:10.1121/1.415223

[9] Fenlon, F. H., "A Recursive Procedure for Computing the Nonlinear Spectral Interactions of Progressive Finite-Amplitude Waves in Nondispersive Fluids," *Journal of the Acoustical Society of America*, Vol. 50, No. 5B, 1971, pp. 1299–1312. doi:10.1121/1.1912766

[10] Pishchal'nikov, Y. A., Sapozhnikov, O. A., and Khokhlova, V. A., "A Modification of the Spectral Description of Nonlinear Acoustic Waves with Discontinuities," *Acoustical Physics*, Vol. 42, No. 3, 1996, pp. 362–367.

[11] Duchon, C. E., "Lanczos Filtering in One and Two Dimensions," *Journal of Applied Meteorology*, Vol. 18, No. 8, 1979, pp. 1016–1022. doi:10.1175/1520-0450(1979)018<1016:LFIOAT>2.0.CO;2

[12] Cleveland, R. O., Chambers, J. P., Bass, H. E., Raspet, R., Blackstock, D. T., and Hamilton, M. F., "Comparison of Computer Codes for the Propagation of Sonic Boom Waveforms Through Isothermal Atmospheres," *Journal of the Acoustical Society of America*, Vol. 100, No. 5, Nov. 1996, pp. 3017–3027. doi:10.1121/1.417113

[13] Viswanathan, K., "Does a Model Scale Nozzle Emit the Same Jet Noise as a Jet Engine," *AIAA Journal*, Vol. 46, No. 2, 2008, pp. 336–355.

doi:10.2514/1.18019
[14] Schmitz, F. H., and Yu, Y. H., "Helicopter Impulsive Noise: Theoretical and Experimental Status," *Journal of Sound and Vibration*, Vol. 109, No. 3, 1986, pp. 361–422. doi:10.1016/S0022-460X(86)80378-9
[15] Boxwell, D. A., Yu, Y. H., and Schmitz, F. H., "Hovering Impulsive Noise: Some Measured and Calculated Results," *Vertica*, Vol. 3, No. 1, 1979, pp. 35–45; also NASA CP-2052, 1978, pp. 309–322.
[16] Purcell, T. W., "CFD and Transonic Helicopter Sound," Fourteenth European Rotorcraft Forum, Paper 2, 1988.
[17] Baeder, J. D., Gallman, J. M., and Yu, Y. H., "A Computational Study of Aeroacoustics of Rotors in Hover," *Journal of the American Helicopter Society*, Vol. 42, No. 1, 1997, pp. 39–53. doi:10.4050/JAHS.42.39
[18] Baeder, J. D., "Euler Solutions to Nonlinear Acoustics of Non-Lifting Rotor Blades," *American Helicopter Society and Royal Aeronautical Society International Technical Specialists Meeting: Rotorcraft Acoustics and Rotor Fluid Dynamics*, 1991.
[19] Menounou, P., and Vitsas P. A., "Numerical Investigation of Nonlinear Propagation Distortion Effects in Helicopter Rotor Noise," *Journal of the Acoustical Society of America*, Vol. 126, No. 4, 2009, pp. 1690–1699. doi:10.1121/1.3203916

A. Lyrintzis
Associate Editor